



Microwave properties of epoxy composites with mixed filler carbon nanotubes/BaTiO₃

O. V. Lozitsky¹ · L. L. Vovchenko¹ · L. Y. Matzui¹ · V. V. Oliynyk² · V. V. Zagorodnii²

Received: 14 December 2018 / Accepted: 11 April 2020 / Published online: 28 April 2020
© King Abdulaziz City for Science and Technology 2020

Abstract

The microwave properties of composite materials (CMs) based on epoxy resin and mixed filler carbon nanotubes/barium titanate (CNT/BT) at CNT concentrations up to 5 wt% and 34 wt% of BT were investigated. The complex permittivity of epoxy composites was measured in the frequency range 1–67 GHz via vector network analyzer. The CNT/BT/epoxy composite showed the increase of permittivity with the increase of CNT content in CM. The electromagnetic shielding properties of developed CMs were measured using waveguide spectroscopy in the frequency range from 26 to 37.5 GHz. Increasing of CNT content enhances the conductivity, resulting in an increase of the EMR reflection at the interface air–composite as well as EMR absorption inside of the composite. The increase of the shields' thickness (up to 2.5 mm) leads to the increase of shielding effectiveness for transmission up to 30 dB for sample with 5% CNT content due to higher EMR absorption inside, while the changes of the reflection index versus frequency depend on CNT content and composite thickness. The reflection loss (RL) of composites was calculated for various thicknesses using the complex permittivity and the obtained results show that composite 2 wt% CNT/BT/epoxy exhibits superior absorptive properties in the frequency range 10–67 GHz. The BT primary role in such CMs (with conductive fillers) is to move the percolation threshold further for conductive filler, increasing its real part of permittivity.

Keywords Polymer composites · Barium titanate · Carbon nanotubes · Shielding · Permittivity

Introduction

High-permittivity polymer materials are highly desirable because of their intrinsic advantages of flexibility, durability, easy processing and lightness (Dang et al. 2012). Their current applications include electromagnetic radiation shielding, circuit board, interlayer dielectrics, leakage current controllers, self-current regulators, passive protection, etc. (Dang et al. 2008; Toner et al. 2012; Ramajo et al. 2010).

Numerous studies have shown that higher dielectric constant can be obtained by adding fillers with dielectric constant, higher than one of the polymer matrix (Ji et al.

2017). As for the type of filler, conductive fillers are able to bring high dielectric constant, but low breakdown strength and high dielectric loss (Dang et al. 2013). It is well known that bulk carbon materials possess a very high conductivity, resulting in mismatch impedance, thereby inducing very limited microwave absorption (Zhao et al. 2012; Wang et al. 2013). Therefore, carbon nanotubes (CNTs) are instead commonly used as filler for CNT/polymer composite microwave absorbers (Mdarhri et al. 2008). Heterostructure-based CNT electromagnetic (EM) absorbers with good impedance matching have been fabricated, indicating that it could be an effective way to optimize the EM parameters and enhance the absorption (Zhou et al. 2013; Boudida et al. 1998). However, CNTs are often in bundles or entangled because of very strong van der Waals attractions between them, which contributed to the current bottleneck to their applications (Ajayan et al. 2000).

Ferroelectric ceramic particles, like BaTiO₃ (BT), are widely used to increase the permittivity of polymer composites because of their own high permittivity and low dielectric loss (Rao et al. 2002; Subodh et al. 2009). However, the

✉ O. V. Lozitsky
Olozitsky@gmail.com

¹ Department of Physics, Taras Shevchenko National University of Kyiv, Volodymyrska str., 64/13, Kiev 01601, Ukraine

² Department of Radiophysics, Electronics, and Computer Systems, Taras Shevchenko National University of Kyiv, Volodymyrska str., 64/13, Kiev 01601, Ukraine

ability of spherical particles to increase the permittivity is small at low volume fractions, according to the rule of mixtures (Sihvola and Alanen 1991). Higher volume fractions lead to increased dielectric constant, but also to a reduction in electrical breakdown strength and mechanical properties (Bai et al. 2000; Cheng et al. 2007). Composites with high aspect ratio fillers are predicted to exhibit higher permittivity at lower filler content (Sihvola and Alanen 1991), thus potentially maintaining the mechanical properties and dielectric breakdown strength (Cheng et al 2007).

The addition of barium titanate particles was found to influence the dielectric properties of the three-component (nanoscale BT–MWCNT)/PVDF nanocomposites significantly, decreasing the conductivity when the content of nanoscale BT concentration was 5 vol.% (Yao et al. 2010). Research of one-dimensional CNT/BaTiO₃/PANI multiphase heterostructure composite has been conducted and the composites showed the best reflection loss of –28.9 dB at 10.7 GHz with a thickness of 3 mm, and a frequency bandwidth less than –20 dB was observed from 10 to 15 GHz (Ni et al. 2015).

This study reports the results of the investigation of electromagnetic interference (EMI) shielding properties of three-phase CNT/BaTiO₃/epoxy CMs. This includes permittivity measurements at frequencies from 1 to 67 GHz, reflection and transmission spectra at frequencies 26–37.5 GHz. Also, the effect of BaTiO₃ on dielectric permittivity compared to pure CNT is presented and discussed.

Experimental

MWCNTs (obtained from Cheap Tubes Inc. company, length 10–30 μm, outer diameter 10–30 nm) and BaTiO₃ ultradisperse powder were used as fillers for the polymer. The average size of dielectric ultradisperse particles of BaTiO₃ was 400 nm.

Low-viscosity epoxy resin Larit285 (L285) [viscosity of 600/900 mPa s, density of 1.18–1.23 g/cm³ (at 25 °C)] with hardening agent H285 (viscosity of 50/100 mPa s) was used as a polymer matrix.

CNT/BaTiO₃/L285 CMs with 1, 2, 3, 4 and 5 wt% of CNTs were fabricated by the method of mixing in solution with additional sonication. At first, the necessary amount of epoxy resin was pre-dissolved with acetone. Next, BT and CNTs fillers were introduced into solution and sonication in BAKU ultrasonic bath with the frequency of 40 kHz and power of 50 W was applied for 2 h. At the next stage, after evaporation of acetone, the curing agent H285 was added in an amount of 40% of L285 weight. The content of BT in CMs was 34.5 wt%.

Fillers distribution in polymer matrix was investigated using optical microscope MIKMED-1 equipped with digital

camera ETREK DCM-510. Permittivity measurements were performed in the frequency range 1–67 GHz, using Keysight Agilent PNA, and a coaxial waveguide. Microwave measurements of shielding effectiveness (EMR transmission index T) and standing wave ratio on voltage (SWR) (related to EMR reflection index R) were performed in the frequency range of 26–37.5 GHz using automated setups based on the scalar network analyzer P2–65. The principle of the method is based on separate detections of the incident and reflected waves. To test the degree of interaction between microwaves and the polymer composites being studied, the specimens were fabricated as rectangular prisms and placed in the waveguide cross section. Reflection index R can be determined from measured SWR, and shielding effectiveness SE_T (in dB) is related to the measured EMR transmission index T using the following equations:

$$R = \left(\frac{\text{SWR} - 1}{\text{SWR} + 1} \right)^2, \quad (1)$$

$$SE_T = 10 \log T, \quad (2)$$

where $R = |E_R/E_I|^2$, $T = |E_T/E_I|^2$, E_I , E_R , E_T are the electric field strengths of the incident, reflected, and transmitted waves, respectively.

EMR absorption A , reflection R and transmission T indices are interrelated by the equation of energy balance (Vovchenko et al. 2011; Wang and Zhao 2013):

$$A + T + R = 1. \quad (3)$$

Results and discussion

Optical microscopy

Figure 1 presents the optical images of BT/epoxy composite and three-phase composites CNT/BT/epoxy. A uniform distribution of ultradisperse BT particles in the epoxy matrix is observed.

For the composites with up to 3 wt% of CNT, uniform distribution of both BT and CNTs fillers in the composite was observed. The increase of CNT content up to 5wt% in CM interferes with the study of filler distribution; however, as it is seen, the approximately uniform distribution of CNT and BT fillers at microscale remained, although the CNT particles tend to agglomerate more, forming extended clusters.

DC electrical conductivity

The data on DC electrical conductivity for CNT/BT/L285 CMs samples filled with 34.5 wt% of BT and variable content of CNT are presented in Table 1.

To display the effect of BT on the conductivity for the investigated CMs, Fig. 2a presents the conductivities of

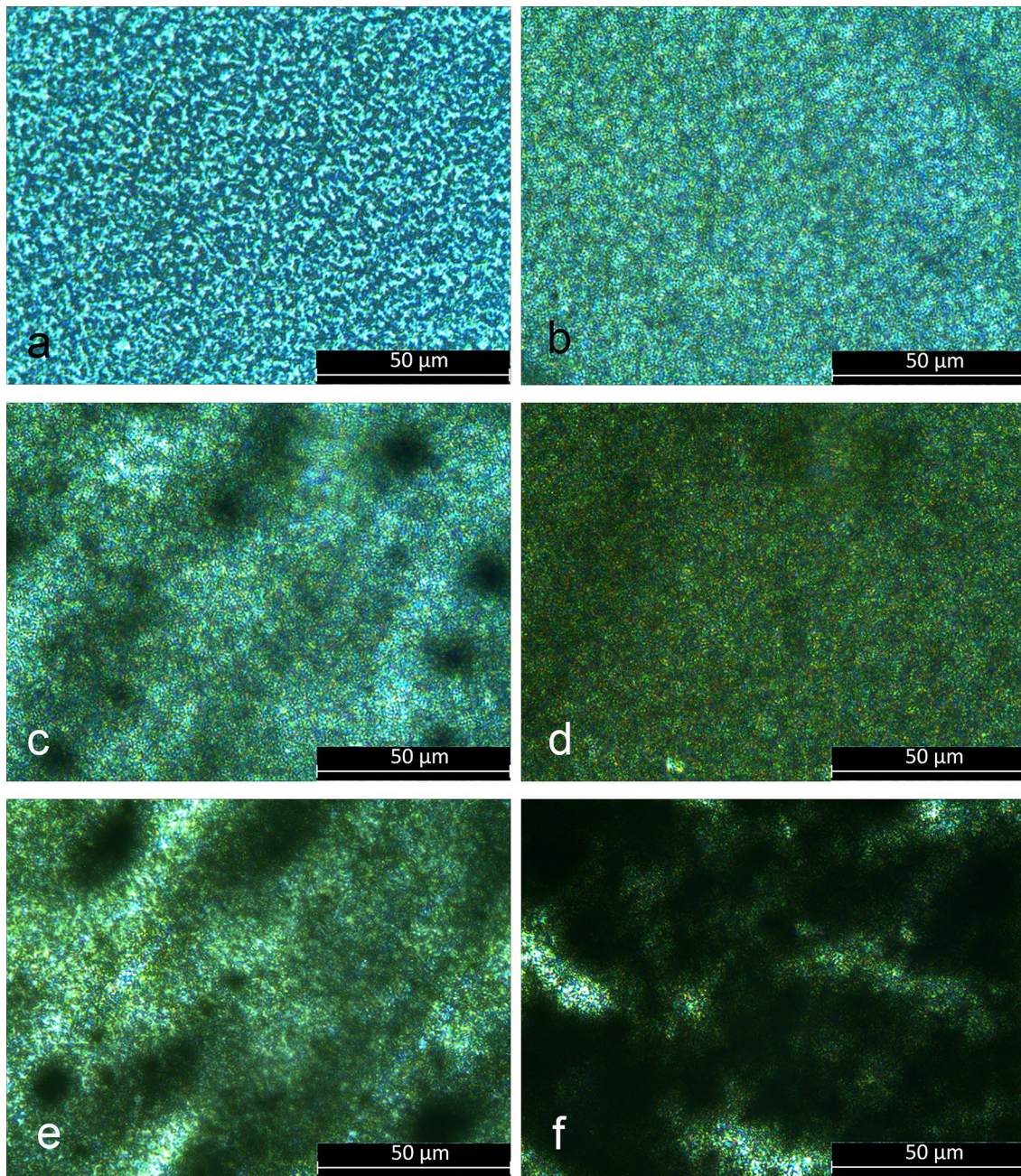


Fig. 1 Optical images of CMs BT/L285 (a), CNT/BT/L285 with 1 wt% CNT (b), 2 wt% CNT (c), 3 wt% CNT (d), 4 wt% CNT (e), 5 wt% CNT (f)

CNT/BT/L285 and CNT/L285 CMs with CNT contents from 0 to 5 wt%. We can see that BT leads to an increase of conductivity at high CNT contents, contrary to what was expected. It is possible that CNT's interlaced nature and non-cylindrical shape causes the spherical BT particles to fill the gaps between the CNTs without preventing contact between them in formed CNT electroconductive clusters. On the other hand, the presence of BT particles

may improve the dispersion of CNT in the epoxy matrix and reduce the aggregation of CNTs in CMs, so the more conductive pathways are formed and electrical conductivity is increased. It should be noted that our recent similar research, using graphite nanoplatelets (GNPs) instead of CNTs, did not display such effect and BT did reduce conductivity in GNP/BT/L285 CMs compared to GNP/L285 CMs (Fig. 2b) (Lozitsky et al. 2018).

Permittivity of the composites

In Fig. 3, the frequency dependencies of permittivity are presented, which were measured in the range of 1–67 GHz, using the Nicolson-Ross-Weir method. Along with broadband increase of real permittivity part with CNT content, the local maxima for $\tan\delta$ is observed, which shifts to lower frequencies as CNT content increases (at ~43 GHz for 1%, ~10 GHz for 3% and ~4 GHz for 5 wt% CNT).

Figure 4 shows the CNT content dependence of permittivity and loss tangent of CNT/BT/L285 composites at the

frequency 35 GHz. The increase of CNT content leads to increased permittivity as a result of the larger capacity of the material which is created by CNT particles separated by epoxy resin. As indicated by the graphs, BT does not affect the real part of permittivity significantly and the effect on loss tangent is inconsistent. Such behavior might be explained by the interlaced structure of CNTs, rather than the cylindrical one, so BT particles do not prevent contact between CNTs as was initially expected and thus the specific electrical capacity of a sample does not increase leading to relatively unchanged permittivity.

Table 1 DC conductivity and porosity of CNT/BT/L285 samples

Composite	BaTiO ₃ (wt%)	CNT (wt%)	Density (g/cm ³)	Porosity	σ_{DC} (S/m)
0CNT/BT/L285	34.5	0	1.40	0.12	2.0×10^{-11}
1CNT/BT/L285	34.5	1	1.45	0.09	2.04×10^{-5}
2CNT/BT/L285	34.5	2	1.45	0.10	2.70×10^{-6}
3CNT/BT/L285	34.5	3	1.41	0.13	2.65×10^{-4}
4CNT/BT/L285	34.5	4	1.49	0.09	1.40×10^{-3}
5CNT/BT/L285	34.5	5	1.42	0.14	5.25×10^{-3}

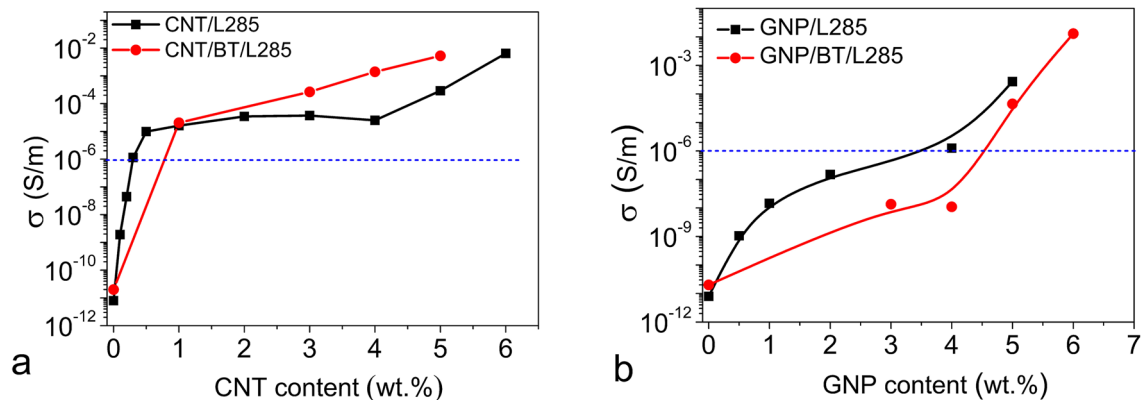


Fig. 2 DC conductivity of CNT/L285, CNT/BT/L285 (a) and GNP/L285, GNP/BT/L285 CMs (b)

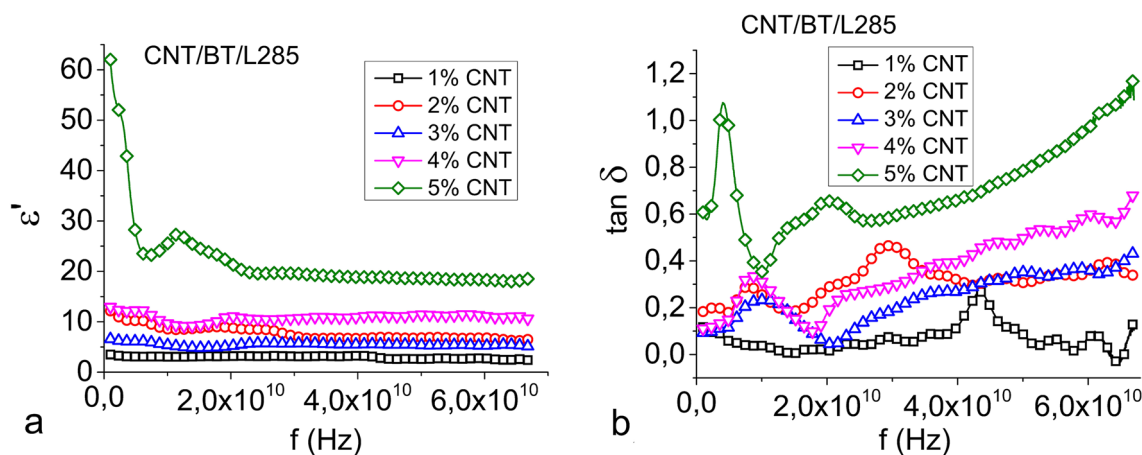


Fig. 3 Real (a) and imaginary (b) parts of permittivity and loss tangent versus frequency of CNT/BT/L285 CMs

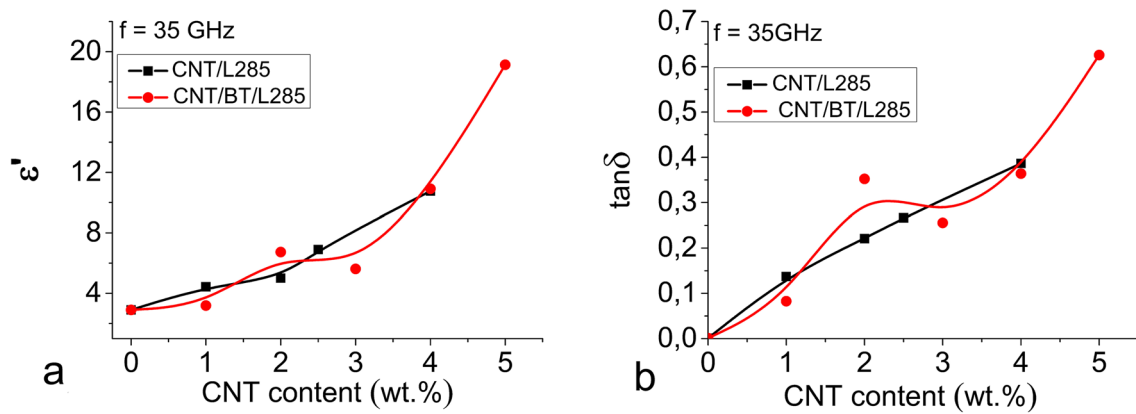


Fig. 4 The real part of permittivity (a) and loss tangent (b) versus content of CNT

Shielding properties of CNT/BT/L285 CMs in Ka band

Measurements of shielding properties were conducted in the range 26–37.5 GHz, where EMR reflection index R and shielding effectiveness for transmission (SE_T) were determined. Oftentimes, it is more convenient to present the shielding properties of a material in terms of shielding effectiveness due to reflection (SE_R) and absorption (SE_A) in addition to transmission, as it clearly shows which process of EMR attenuation is dominant. These values are related as follows (Maiti and Khatua 2016):

$$SE_T = SE_A + SE_R + SE_I; \quad SE_R = 10\log(1 - R); \quad SE_A = 10\log\left(\frac{T}{1 - R}\right), \quad (4)$$

where R and T are energy reflection and transmission indices, respectively.

$$SE_T = 10\log|T| = -20\log|e^{\gamma d}| - 20\log\left|\frac{(1+n)^2}{4|n|}\right| - 20\log\left|1 - \frac{(1-n)^2}{(1+n)^2}e^{-2\gamma d}\right| = SE_A + SE_R + SE_I, \quad (5)$$

The results for SE_T , SE_R and SE_A are presented in Fig. 5 (sample thickness is 1.0 mm) and Fig. 6 (sample thickness is 2.5 mm).

While the SE_T and SE_A absolute values increase monotonically with the increase of CNT content, we see that SE_R is at its lowest (least reflection) at 3 wt% of CNT for 1 mm layer and at 2 wt% of CNT for 2.5 mm sample. These properties can be understood if we consider that permittivity determines impedance mismatch of the interfaces, in this case, air–CM and CM–air. The larger the mismatch, the larger will the fraction of incident wave amplitude be reflected at the interface. When the shields’ permittivity is low, the EMR passes through the shield without much reflection, but when the permittivity is high, the larger part of radiation is

reflected at the first air–CM interface. The larger reflection of 1 mm samples with 1 and 2 wt% of CNT could be attributed to interference conditions between air–CM and CM–air interfaces amplifying the reflected radiation (Fig. 5b), while 2.5 mm samples with 1 and 2 wt% of CNT have the interference attenuate the reflected radiation, indicated by the least reflection (Fig. 6b).

Figure 7 presents the values of SE_T , SE_R and SE_A depending on the CNT content.

The EMR shielding efficiency SE_T (in dB) of the shield is determined by electrodynamic parameters of the mate-

rial and can be described by the following expression (Joo and Lee 2000; Liu et al. 2007):

where $n = k_z/k_0$ is the complex refractive index; $k_0 = 2\pi/\lambda_0$ is the wavenumber in free space, $\lambda_0 = C_0/f$; λ_0 and f are the wavelength and frequency; $C_0 = 3 \times 10^8$ m/s; $k_z = k_0\sqrt{\epsilon_r^*\mu_r^*}$; $\gamma = \alpha + i\beta$ is EMR complex propagation constant (β is the phase constant, α is the absorption index); d is the shielding material thickness.

As it follows from Eq. (5), the increase of complex permittivity and thickness of composite sample may lead to the increase of EMR shielding efficiency SE_T and explain the observed experimental spectra for EMR reflection, absorption and transmission.

The obtained experimental dependence of permittivity versus frequency for the studied composites allows it to estimate their absorbing properties in a wide microwave

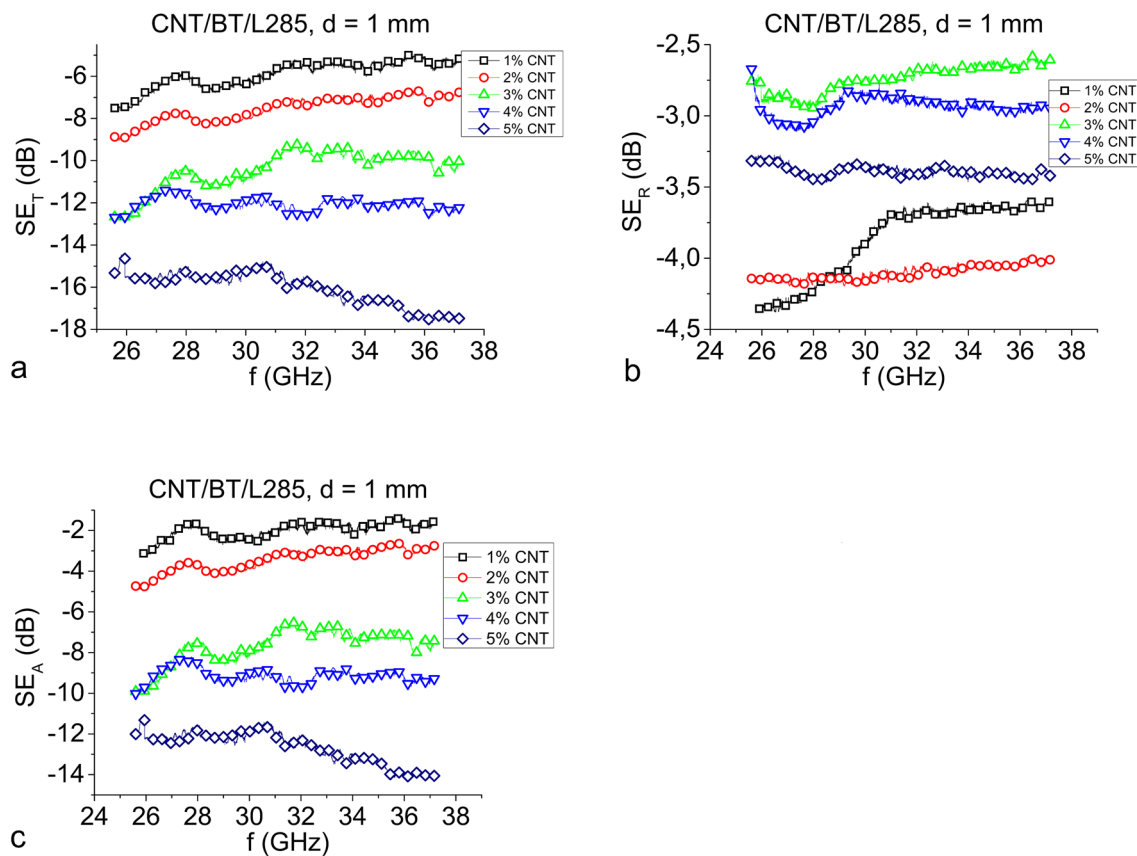


Fig. 5 SE_T (a), SE_R (b) and SE_A (c) spectra for CNT/BT/L285 sample with 1 mm thickness

frequency range. For this case, the composite sample backed by a metal plate is considered. The reflection loss, which is related to the absorptive ability of a composite, may be described by the following expression (Dosoudil et al. 2010):

$$RL = 20 \log \left| \frac{Z_{in} - Z_0}{Z_{in} + Z_0} \right|, \quad (6)$$

where $Z_{in} = Z_0 \sqrt{\mu_r / \epsilon_r} \tanh(\gamma d)$ is the input wave impedance at the air–CM interface, and $Z_0 = \sqrt{\mu_0 / \epsilon_0} = 377 \Omega$ is the free-space wave impedance.

Based on the electromagnetic parameters (the complex values of permittivity and permeability), the RL can be calculated for the given frequency with various thicknesses according to (6).

To present how change in sample thickness may affect absorption, the modeling of reflection loss for a sample backed by a metal plate was conducted. The modeling method was the transmission line method. The metal plate causes any radiation that penetrated the sample to reflect, so transmission can be neglected. Thus by observing the reflection index, we can determine how absorptive a material is. Figure 8 presents data on reflection loss for samples

CNT/BT/L285 with 1, 2, 3 and 5 wt% of CNT at thicknesses ranging from 1 to 2.5 mm. Arrows on the graphs depict the motion of reflection minima with an increase of sample thickness.

The observed minimum in reflection loss means that the microwave can be dissipated by a so-called “geometrical effect” when the thickness of absorbers satisfies the following equation and the reflected waves are totally canceled in the air–absorber interface (Hu et al. 2018; Vovchenko et al. 2016):

$$d_m = \frac{n}{4} \cdot \frac{C_0}{f_m \cdot \sqrt{|\mu_r \cdot \epsilon_r|}}, \quad n = 1, 3, 5, \quad (7)$$

where f_m is the matching frequency that corresponding to RL_{min} , and d_m is the matching thickness of the sample.

We can see that for samples with 1 wt% of CNT, the increase of thickness does not affect the position of reflection minima, rather changing the values, and one thickness can be the best for absorption at one frequency but not for the other. However, regardless of these considerations, the amount of CNT this low causes most of EMR energy to pass through the sample, reflect from the metal plate and

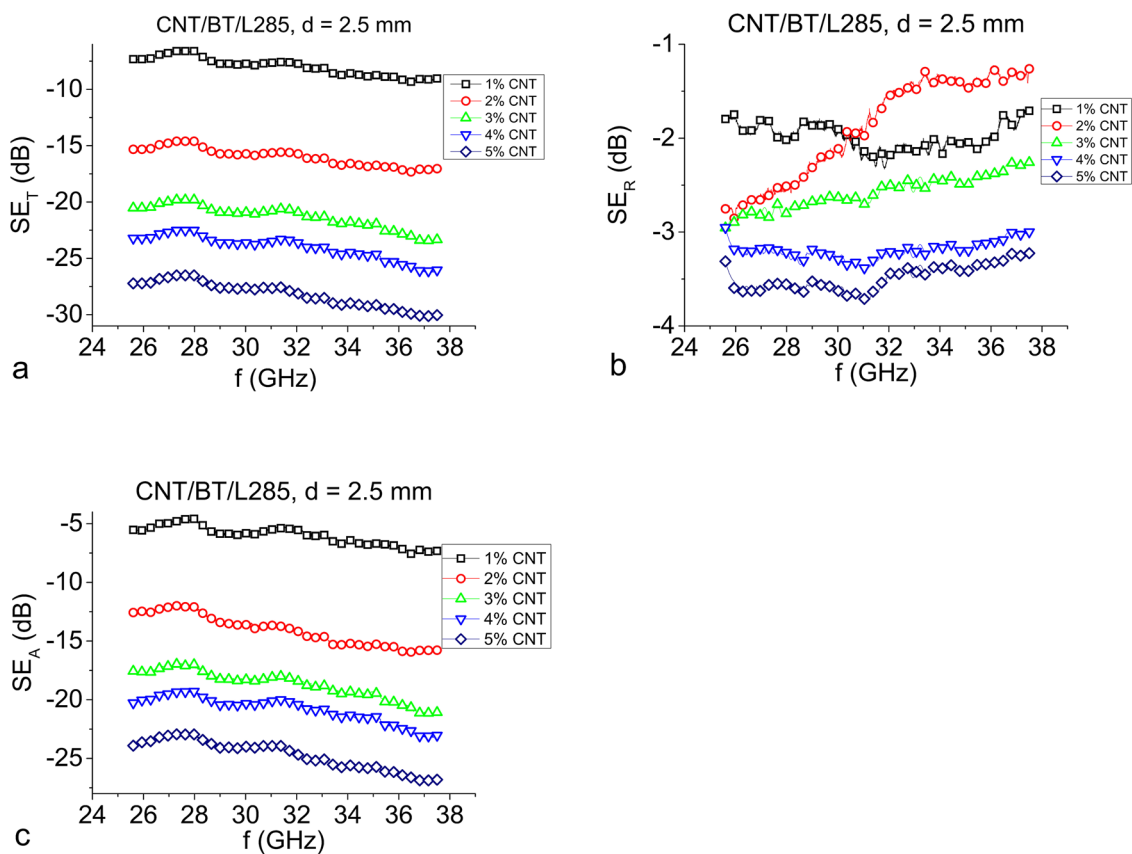


Fig. 6 SE_T (a), SE_R (b) and SE_A (c) spectra for CNT/BT/L285 samples with 2.5 mm thickness

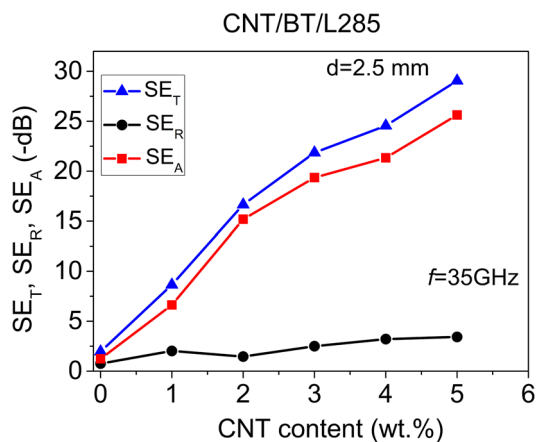


Fig. 7 SE_T , SE_R and SE_A versus CNT content in CNT/BT/L285 samples at 35 GHz

leave the sample without much loss, so it is not the best solution for absorbing material at these frequencies in a solid sample, but may be used in composite structure that aims to trap a radiation inside, like sandwich structures or photonic/quasi-photonic crystals.

It turned out that 2 and 3 wt% of CNT provide the largest absorption in range 10–65 GHz. The figures show that increasing the thickness shifts the absorption minima to lower frequencies and changes the depth of the minima, i.e., the matching frequency decreases with the increase in the absorber thickness in agreement with the relation (7). In some cases, such changes can yield particularly deep band gaps. A sample with 2 wt% CNT, in 1 mm, for example, exhibited a 39 dB absorption level at 26.5 GHz frequency and the effective absorption bandwidth corresponding to reflection loss (RL) below -10 dB reaches up to ~ 10 GHz. Such absorption is likely caused by interference between reflected waves from the air–sample and sample–metal boundaries such that wave phases are shifted by an odd multiple of $\frac{\pi}{2}$, largely canceling the reflecting radiation. Comparing Fig. 8d with Fig. 8b, c, it can be found that for the samples with 5 wt% of CNT, the effective absorption bandwidth and depth of band gaps are reduced. Thus, it may be concluded that these composites are not the best standalone absorbing materials, since the larger part of microwave radiation is reflected from the first air–CM interface, so the smaller part of EMR has the chance to be absorbed inside. However, it can be seen that increasing the thickness shifts the reflection minima to lower

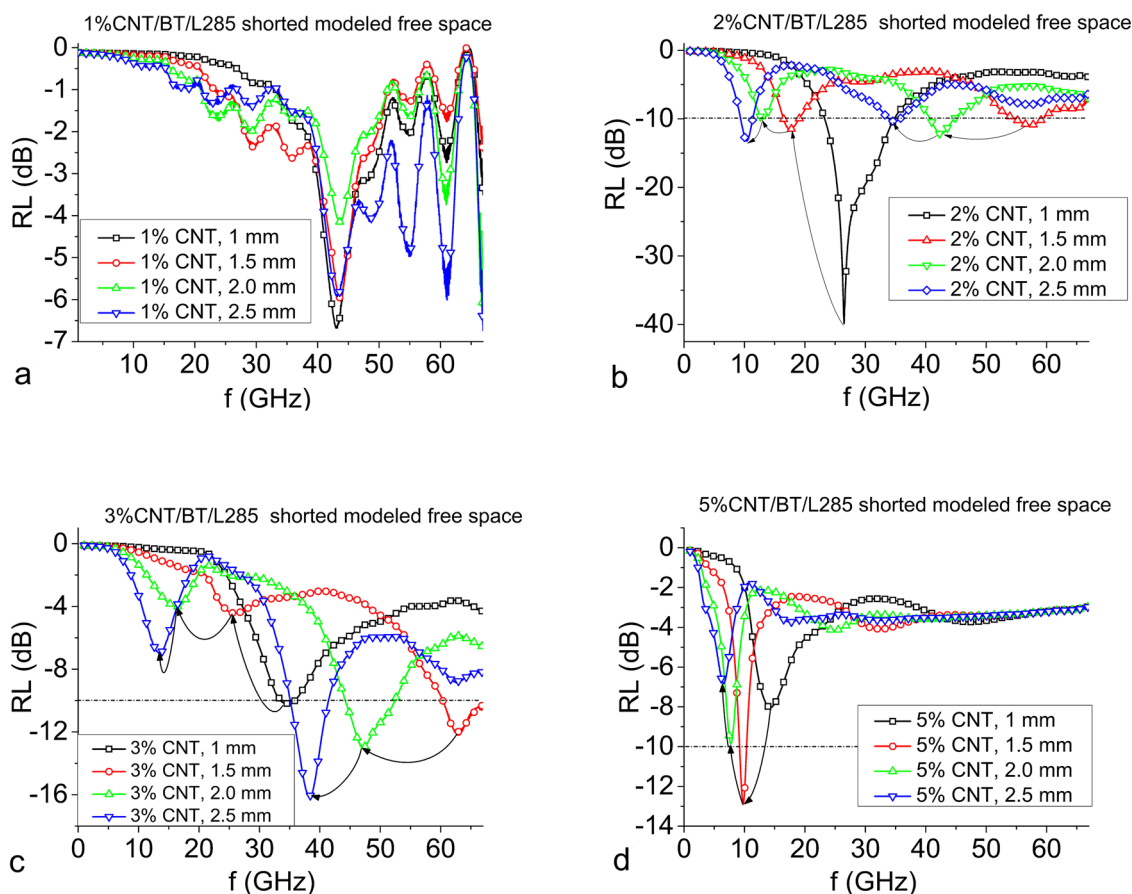


Fig. 8 Modeled reflection loss versus frequency of CNT/BT/L285 samples with 1 (a), 2 (b), 3 (c), 5 (d) wt% of CNT with sample thicknesses 1–2.5 mm

frequencies, and in general, deeper minima are focused at around 10 GHz. If one aims to obtain a band gap there, then such CNT content may be suitable.

Naturally, to use interference conditions for absorption purposes, the samples must be produced with high precision of thickness and permittivity that is not always available, since permittivity may vary substantially even for samples with same composition and manufacturing conditions. Thus, an important task is to develop a material that not only allows high permittivity without being conductive, but also one that can produce such permittivity consistently at a given composition (filler type and content). The determination of parameters of materials that will yield the necessary shielding properties is a separate task, which may be solved by mathematical optimization.

Conclusions

The CNT/BT/L285 composites (CMs) have been prepared with CNT contents ranging from 1 to 5 wt%. An optical microscopy has shown a uniform distribution of BT and

CNT particles at microscale, but samples with 4 and 5 wt% of CNT have shown an agglomeration of CNT particles in extended clusters.

DC conductivity measurements have shown larger conductivity of CNT/BT/L285 CMs, compared to CNT/L285 CMs, possibly caused by the interlaced structure of CNT clusters and non-cylindrical shape of CNTs themselves.

Permittivity measurements in the frequency range 1–67 GHz have displayed no consistent change of complex permittivity, suggesting that CNT/BT/L285 CMs perform similarly to CNT/L285 CMs as shielding materials, possibly due to the same reasons that caused the increased conductivity: interweaved structure of CNTs and deviation from cylindrical shape of CNTs.

Shielding measurements at shields' thicknesses of 1 and 2.5 mm were conducted for Ka-band and displayed an increase of attenuation with the increase of CNT content and lowest values of shielding due to reflection SE_R at 3 wt% of CNT for the sample with 1 mm thickness and at 2 wt% of CNT for the sample with 2.5 mm thickness, suggesting that wave interference on air–CM and CM–air interfaces takes

place amplifying or negating the reflected radiation at certain CNT contents.

A modeling of absorption properties was performed for samples with thickness 1–2.5 mm, backed by a metal plate. A composite sample 2 wt% CNT/BT/L285 has shown superior absorptive properties in the frequency range 10–65 GHz. Therefore, it can be concluded that the excellent microwave absorption properties of 2% CNT/BT/epoxy composite at certain frequencies may come from the contribution of “geometrical effect” when the reflected waves are totally canceled in the air–absorber interface at a certain matching thickness of the sample.

References

- Ajayan PM, Schadler LS, Giannaris C, Rubio A (2000) Single-walled carbon nanotube-polymer composites: strength and weakness. *Adv Mater* 12:750–753
- Bai Y, Cheng ZY, Bharti V, Xu H, Zhang QM (2000) High-dielectric-constant ceramic-powder polymer composites. *Appl Phys Lett* 76:3804
- Boudida A, Beroual A, Brosseau C (1998) Permittivity of lossy composite materials. *J Appl Phys* 83:425–431
- Cheng KC, Lin CM, Wang SF, Lin ST, Yang CF (2007) Dielectric properties of epoxy resin-barium titanate composites at high frequency. *Mater Lett* 61:757
- Dang ZM, Yu YF, Xu HP, Bai J (2008) Study on microstructure and dielectric property of the BaTiO₃/epoxy resin composites. *Compos Sci Technol* 68:171178
- Dang ZM, Yuan JK, Zha JW, Zhou T, Li ST, Hu GH (2012) Fundamentals, processes and applications of high-permittivity polymer matrix composites. *Prog Mater Sci* 57(4):660–723
- Dang ZM, Yuan JK, Yao SH, Liao RJ (2013) Flexible nanodielectric materials with high permittivity for power energy storage. *Adv Mater* 25:6334–6365
- Dosoudil R, Usáková M, Franek J, Sláma J, Grusková A (2010) Particle size and concentration effect on permeability and EM-wave absorption properties of hybrid ferrite polymer composites. *IEEE Trans Magn* 46:436
- Hu R, Tan G, Gu X, Chen S, Wu C, Man Q, Chang C, Wang X, Li RW, Che S, Jiang L (2018) Electromagnetic and microwave-absorbing properties of Co-based amorphous wire and Ce₂Fe₁₇N_{3-δ} composite. *J Alloy Compd* 730(5):255–260
- Ji W, Deng H, Fu Q (2017) Heterogeneous filler distribution in polymeric capacitor films: an efficient route to improve their dielectric properties. *Compos Sci Technol* 151:131–138
- Joo J, Lee CY (2000) High frequency electromagnetic interference shielding response of mixtures and multilayer films based on conducting polymers. *J Appl Phys* 8:513
- Liu Z, Bai G, Huang Y, Ma Y, Du F, Li F, Guo T, Chen Y (2007) Reflection and absorption contributions to the electromagnetic interference shielding of single-walled carbon nanotube/polyurethane composites. *Carbon* 45:821
- Lozitsky OV, Vovchenko LL, Matzui LY, Milovanov YS (2018) Dielectric properties of epoxy composites with mixed fillers including graphite nanoplatelets/BaTiO₃. *Mol Cryst Liq Cryst*. <https://doi.org/10.1080/15421406.2018.1542086>
- Maiti S, Khatua BB (2016) Graphene nanoplate and multiwall carbon nanotube-embedded polycarbonate hybrid composites: high electromagnetic interference shielding with low percolation threshold. *Polym Compos* 37:2058
- Mdarhri A, Carmona F, Brosseau C, Delhaes P (2008) Direct current electrical and microwave properties of polymer-multiwalled carbon nanotubes composites. *J Appl Phys* 103:054303
- Ni QQ, Zhu YF, Yu LJ, Fu YQ (2015) One-dimensional carbon nanotube@barium titanate@polyaniline multiheterostructures for microwave absorbing application. *Nanoscale Res Lett* 10:174
- Ramajo L, Reboredo MM, Castro MS (2010) BaTiO₃-epoxy composites for electronic applications. *Int J Appl Ceram Technol* 7:444451
- Rao Y, Ogitani S, Kohl P, Wong CP (2002) Novel polymer-ceramic nanocomposite based on high dielectric constant epoxy formula for embedded capacitor application. *J Appl Polym Sci* 83:1084
- Sihvola A, Alanen E (1991) Studies of mixing formulae in the complex plane. *IEEE Trans Geosci Remote Sens* 29:679
- Subodh G, Deepu V, Mohanan P, Sebastian M (2009) Dielectric response of high permittivity polymer ceramic composite with low loss tangent. *Appl Phys Lett* 95:062903
- Toner V, Polizos G, Manias E, Randal CA (2012) Epoxy-based nanocomposites for electrical energy storage. I: effects of montmorillonite and barium titanate nanofillers. *J Appl Phys* 108:074116
- Vovchenko LL, Matzui LY, Oliynyk VV, Launetz VL (2011) The effect of filler morphology and distribution on electrical and shielding properties of graphite-epoxy composites. *Mol Cryst Liq Cryst* 535:179–188
- Vovchenko LL, Matzui LY, Brusyllovets O, Oliynyk VV, Launetz VL, Shames A, Yakovenko O, Skoryk N (2016) Synthesis and properties of ferrite nanopowders for epoxy-barium hexaferrite-nanocarbon composites for microwave applications. *Mat-wiss u Werkstofftech* 47(2–3):139–148
- Wang Z, Zhao GL (2013) Microwave absorption properties of carbon nanotubes-epoxy composites in a frequency range 2–20GHz. *Open J Compos Mater* 3:17
- Wang ZJ, Wu L, Zhou JG, Cai W, Shen BZ, Jiang ZH (2013) Magnetite nanocrystals on multiwalled carbon nanotubes as a synergistic microwave absorber. *J Phys Chem C* 117:5446–5452
- Yao SH, Yuan JK, Dang ZM, Bai J (2010) High dielectric performance of three-component nanocomposites induced by a synergetic effect. *Mater Lett* 64:2682
- Zhao CY, Zhang AB, Zheng YP, Luan JF (2012) Electromagnetic and microwave-absorbing properties of magnetite decorated multiwalled carbon nanotubes prepared with poly(*N*-vinyl-2-pyrrolidone). *Carbon Res Bull* 47:217–221
- Zhou XB, Shen L, Li L, Zhou SH, Huang TM, Hu CF et al (2013) Microwave sintering carbon nanotube/Ni_{0.5}Zn_{0.5}Fe₂O₄ composites and their electromagnetic performance. *J Eur Ceram Soc* 33:2119–2126

Publisher's Note Springer Nature remains neutral with regard to jurisdictional claims in published maps and institutional affiliations.